

## Star-drops formed by periodic excitation and on an air cushion – A short review

P. Brunet<sup>1,a</sup> and J.H. Snoeijer<sup>2,b</sup>

<sup>1</sup> Institut d'Électronique de Microélectronique et de Nanotechnologies, UMR CNRS 8520, Avenue Poincaré, BP. 60069, 59652 Villeneuve d'Ascq, France

<sup>2</sup> Physics of Fluids Group and J.M. Burgers Centre for Fluid Dynamics, University of Twente, PO Box 217, 7500 AE Enschede, The Netherlands

Received 21 January 2011 / Received in final form 25 January 2011  
Published online 9 March 2011

**Abstract.** When simply put on a solid, a liquid drop usually adopts the shape of a spherical cap or a puddle depending on its volume and on the wetting conditions. However, when the drop is subjected to a periodic field, a parametric excitation can induce a transition of shape and can break the drop's initial axial symmetry, provided that the pinning forces at the contact-line are weak enough. Therefore, a standing wave appears at the drop interface and induces a periodic motion, with a frequency that equals half the excitation frequency. In the first part, we review the different situations where star drops can be generated from various types of periodic excitations. In the second part, we show that similar star drops can occur in a much less intuitive fashion when the drop is put on an air cushion, where no periodic motion is imposed *a priori*. Preliminary experiments as well as theoretical clues for a hydrodynamic interpretation, suggest that the periodic vibration is due to an inertial instability in the air layer below the drop.

### 1 Introduction

In the search for the dynamical properties of liquids drops, which are more and more used for discrete microfluidics applications, various studies have been devoted to the determination of their eigenmodes with respect to the response to external forces. In the linear regime and for inviscid spherical drops, the resonance frequency has been theoretically predicted a long time ago by Rayleigh and Lamb [1]:

$$f_n = \left( \frac{n(n-1)(n+2)\gamma}{3\pi\rho V} \right)^{1/2} \quad (1)$$

$$= \frac{1}{2\pi} \left( \frac{n(n-1)(n+2)\gamma}{\rho R^3} \right)^{1/2} \quad (2)$$

<sup>a</sup> e-mail: philippe.brunet@univ-lille1.fr

<sup>b</sup> e-mail: J.H.Snoeijer@tnw.utwente.nl

in which  $f_n$  denotes the resonance frequency of the  $n^{\text{th}}$  mode of oscillation,  $V$  is the drop volume,  $R$  its radius,  $\gamma$  and  $\rho$  the liquid surface tension and density.

In practice, however, the situation is much more complex for a number of reasons: (1) the shape is not spherical, for instance if the drop is put on a solid substrate (sessile drop); (2) the drop deformations are large enough to depart from the range of the linear theory; (3) the prescribed vibration is anharmonic. A common way to access these dynamical properties is to put a sessile drop onto a mechanical shaker, subjecting the liquid to an oscillatory inertial force [2–5]. This geometry allows for the observation of a host of phenomena from linear to strongly non-linear behavior, i.e. from surface wave undulations to strong deformations up to atomization [2]. However, an additional degree of complexity appears due to the presence of the contact line, which accounts for the liquid-solid interactions at the microscopic scales. Most of the viscous dissipation occurs in the vicinity of the contact line, and the combination of roughness and chemical heterogeneity of any real surface leads to a pinning force, quantified by a contact-angle hysteresis [6]. The eigen-mode of a drop is strongly influenced by this pinning force [3], but it is possible to remove this complexity by using a low-friction hydrophobic substrate [4]. In this case the drop's eigen frequencies follow a law similar to (2), with a corrective geometrical pre-factor [5, 7] that depends on its shape – from a flattened sphere to a puddle – and on the contact-angle [8].

A drop weakly pinned on its substrate can experience a shape transition from axisymmetric to that of finite azimuthal wave-number, giving it *the shape of a star* (see Fig. 3). This transition happens in various situations where a periodic field (acceleration, magnetic field, ...) can induce a parametric forcing in the drop. Since examinations of the flow inside the drop show more or less regular vortex-like structures [9], this type of instability can be utilized on purpose to induce constant mixing or particle re-suspension. Otherwise, star drops have been observed when levitated on an air cushion, and this situation has numerous applications as well, depending on whether one desires to induce or to avoid shape oscillations. For example in lens manufacture, drops of molten glass can be prevented from contact with a solid substrate [10] by levitating the glass above a porous mould. It is also employed as a viscosimeter for harmful or high-temperature liquids [11]. In the former case, the shape oscillations have to be avoided, whereas in the latter case they are desired.

When the drop is sustained by a gas stream flowing underneath [12], the levitating flow is not *a priori* time-dependent. However, the drop spontaneously exhibits time-periodic oscillations. This suggests a mechanism that originates from an instability in the flow. A similar situation is encountered when the drop levitates above a hot plate. When the temperature of the surface is much larger than the boiling temperature, the liquid experiences a boiling crisis – the so-called ‘Leidenfrost effect’ – where a thin vapour layer insulates the liquid from the substrate and keeps the drop in levitation [13–18]. While it has become apparent that the star shapes come from a parametric forcing, originating from a periodic acceleration field, the mechanism for periodic spontaneous oscillations of the drop is not yet understood. Mechanisms invoking thermal effects are invalidated by the observation of star drops on a ambient temperature air cushion [12, 19], and an analysis only based on viscous lubrication and capillarity is unable to reproduce sustained oscillations [20]. The stability of this air cushion is also crucial for the non-coalescence of droplets on a vibrated bath [21, 22].

In this paper, we review the current literature of the formation of faceted star drops in various experimental situations and we show experimental results of star formations from liquid puddle shaken on a super-hydrophobic substrate (section 2). In the second part (section 3) we review situations of drops levitated on an air cushion that develop similar star shapes, but without any prescribed periodic excitations. We show the first experimental evidence of such stars and our data suggests that their formation indeed originates from a hydrodynamic instability of the air flow.

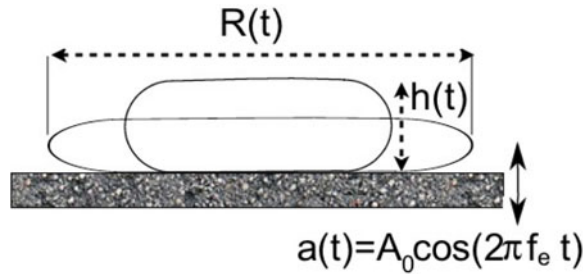


**Fig. 1.** A liquid puddle on a non-wetting substrate vibrated in the vertical direction at a frequency  $f_e$ . Due to a time-periodic acceleration  $a(t)$ , the puddle radius  $R(t)$  and height  $h(t)$  are time-dependent.

## 2 Star drops generated by periodic excitation: A catalogue

### 2.1 General features

Here we give a qualitative understanding of how a drop can generate standing waves, associated to the shape of a star, as a response to a time-periodic excitation. We basically follow the analysis found in the paper by Yoshiyasu et al. [5]. Let us consider the simple case of a large drop (liquid density  $\rho$  and surface tension  $\gamma$ ) sitting on a non-wetting substrate Fig. 1. If the drop volume is large enough, it spreads like a puddle which radius  $R$  is much larger than the height  $h$ . We wish to approach the situation of a non-wetting substrate (contact angle  $\theta$  equal to  $180^\circ$ ), although in practice  $\theta$  is rarely larger than  $160^\circ$ . The height  $h$  is equal to twice the capillary length  $l_c$ :  $h = 2l_c = \sqrt{\frac{4\gamma}{\rho g}}$ , and it ranges between 2 and 3 millimeters for most liquids.

Now, the substrate is periodically vibrated in the vertical direction. Therefore, the drop is subjected to a time-periodic acceleration field  $a(t)$ . The balance between gravity and surface tension, selecting the capillary length  $l_c$  no longer holds. Consequently, one has to build an effective capillary length  $l_c^*$  that is also time dependent, which implies that the height of the puddle ( $h = 2l_c^*$ ) varies periodically:

$$h = \sqrt{\frac{4\gamma}{\rho(g + a(t))}} = \sqrt{\frac{4\gamma}{\rho(g + A_0(2\pi f_e)^2 \cos(2\pi f_e t))}}. \quad (3)$$

Due to the volume conservation of the drop,  $V = \pi R^2 h$ , the radius also fluctuates with a period of  $\frac{1}{f_e}$ .

It can be argued that the eigen frequencies of a liquid puddle on a non-wetting substrate do not differ much from those of a spherical drop described by eq. (2). This is the case when the wetting conditions do not introduce any significant pinning force at the contact-line. If a pinning force would exist, the contact-angle would show a hysteretic behavior, which would prevent any variation of the radius  $R$ , or would lead to stop-and-go variations for  $R$  [3]. By assuming in addition that the radius  $R$  is significantly larger than the height  $h$ , Takaki and Adashi [14] showed that the eigen frequency of the  $n^{\text{th}}$  mode – corresponding to a drop with  $n$  lobes along the azimuthal direction – is equal to:

$$f_n = \frac{1}{2\pi} \left( \frac{n(n^2 - 1)\gamma}{\rho R^3} \right)^{1/2}. \quad (4)$$

It is clear from eq. (3) that the resonance frequency  $f_n$  for the free oscillations are modulated in time. Therefore, this modulation leads to parametric forcing, by analogy

with the classical case of a vertically shaken pendulum [23]. Yoshiyasu et al. show with simple arguments that the equation for the horizontal displacement of the drop periphery  $u(t)$  is governed by an equation similar to the Mathieu equation:

$$\frac{d^2u}{dt^2} + \omega_n^2(1 + \xi \cos(2\pi f_e t))u = 0 \quad (5)$$

with  $\omega_n = 2\pi f_n$  is the pulsation associated to the  $n^{\text{th}}$  mode, and  $\xi = \frac{3\Delta R}{R}$ . It was also verified experimentally that the frequency of the drop oscillations  $f_n$  is equal to half the prescribed frequency  $f_e$ , which is expected for parametric forcing. Consequently, the drop exhibits a standing wave at its periphery, which wavelength  $\lambda$  has to match both the perimeter  $2\pi R$  and the number of lobes  $n$ :  $\lambda = \frac{2\pi R}{n}$ ,  $n$  being fixed by the prescribed frequency:  $f_n = \frac{f_e}{2}$ .

It is worth emphasizing the importance of having a weak pinning force between the drop and the substrate. In the situation where a significant pinning force exists, the substrate oscillations leads to a very different dynamics, as the drop radius stays constant. Instead, it is the contact-angle that fluctuates, at the frequency  $f_e$  [3], due to the vertical oscillation of the drop's center of mass. As the drop radius does not vary over time, no parametric forcing is possible and the drop simply responds harmonically. This also explains why a sessile drop on an oscillatory substrate responds at the frequency of excitation whereas a non-adhesive drop undergoes a parametric instability with a response at half the frequency of excitation.

It is also to be noticed that a similar phenomenon has been recently evidenced on bubbles subjected to ultrasonic forcing [24]. Due to the much weaker mass of bubbles compared to drops, the typical period for resonance is around  $8 \mu\text{s}$  ( $f = 125 \text{ kHz}$ ).

Finally, let us mention that the star shapes are the direct consequence of the peculiar geometry of a flat puddle, i.e. that  $R$  is much larger than  $h$ . The star shapes are much less pronounced for spherical drops, as shown e.g. in [25]. For drop of intermediate volume, between sphere and puddle, the shapes are hybrids, as the lobes and nodes take place in both the azimuthal and the up-down directions.

## 2.2 Experiments on puddles on a vibrating non-wetting substrate

### 2.2.1 A brief history of previous experiments

Putting a puddle on a non-wetting and non-sticky vibrating surface is probably the easiest way to observe star drops. Yoshiyasu et al. [5] carried out the first qualitative experiments, using a teflon plate. The authors pointed out that it is particularly important that the water drop formed a contact angle  $\theta$  larger than  $120^\circ$ . However, Noblin et al. showed that liquid stars – denoted there as “triplons” to refer to the azimuthal deformation of the triple (contact) line – could be observed on a substrate with contact-angle  $\theta$  smaller than  $90^\circ$ , provided that the contact angle hysteresis was small enough (in practice, less than 15 degrees). The only difference is the existence of a threshold in acceleration (or shaking amplitude) below which the contact-line keeps pinned [3,4]. They generalized eq. (5) in the case of solid-like friction, and demonstrated that, above the threshold of contact line depinning, the instability that turns an initial axisymmetric drop to a faceted star drop is associated to an exponential growth of the lobe amplitude versus time. Therefore, this feature contains the signature of a linear instability.

More recent experiments by Okada and Okada [25] produced more quantitative data using a more hydrophobic teflon plate. They especially focused on the mode  $n = 3$ , and produced an existence diagram for this simple mode varying both

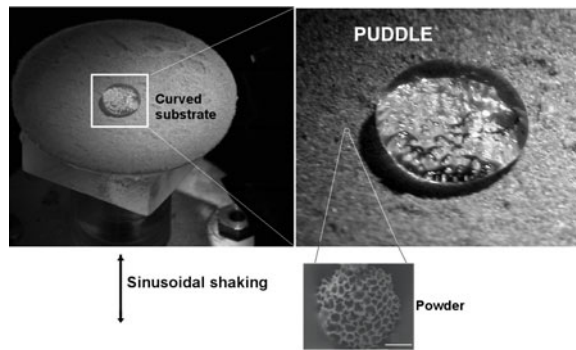


**Fig. 2.** Schematic experimental set-up utilized to generate star drops on a shaken hydrophobic curved substrate. The bottom inset shows a hydrophobic particle used to coat the substrate (the bar scales for  $10\ \mu\text{m}$ ).

amplitude and excitation frequency. They also checked that the response frequency scaled with  $V^{\frac{1}{2}}$  for the same  $n$ , with  $V$  is the drop volume. Finally, it is to be noticed that star drops have recently been observed in the geometry of a large drop sandwiched between two hydrophobic plates shaken vertically [9].

### 2.2.2 Our experiments: The set-up

In order to give a more quantitative picture of the formation of stars, we carry out systematic experiments in a large range of frequency and with different drop volumes. We choose  $V = 100, 200, 500$  and  $1000$  ml, for which water drops adopt the shape of puddles. As a substrate, we fabricate a home-made superhydrophobic surface by spreading a water-repellent powder (Lycopodium) on a layer of adhesive wax. Then, we blow on the powder layer to remove the remaining grains. As a result, we obtain a nearly regular monolayer of powder: the combination of surface roughness and hydrophobic nature of the powder layer ensures a highly water-repellent behavior. Although the superhydrophobic properties deteriorate faster than those of the surfaces mode of micro-pillar arrays or nano-structurations (see [26] for a review), they have a reasonable life-time, suitable for the time of the experiments. The contact angle  $\theta$  was measured to be equal to  $140 \pm 2^\circ$ . When putting a large puddle on the surface, one observed a thin layer of air trapped between the liquid and the substrate which testifies for the strong repellency (see Fig. 2). The hysteresis is very weak and a drop would roll off the surface even for very small tilts. Therefore, we operate in a curved glass surface to keep the drop at the same central location. The whole substrate is shaken vertically using an electromagnetic shaker. The drop dynamics was recorded using a high-speed camera (Phantom V5). The set-up is schematically reproduced in Fig. 2.

### 2.2.3 Results

By varying the drop volume, the amplitude and frequency of the shaking, we are able to generate star drop with  $n$  from 2 up to 15 lobes. Some examples of these stars are presented in Fig. 3. In order to better understand the selection mechanism, we construct phase diagrams for different drop volumes by varying both the frequency  $f_e$  of excitation and the acceleration  $a$  through the amplitude of vibration:  $a = A_0(2\pi f_e)^2$ .

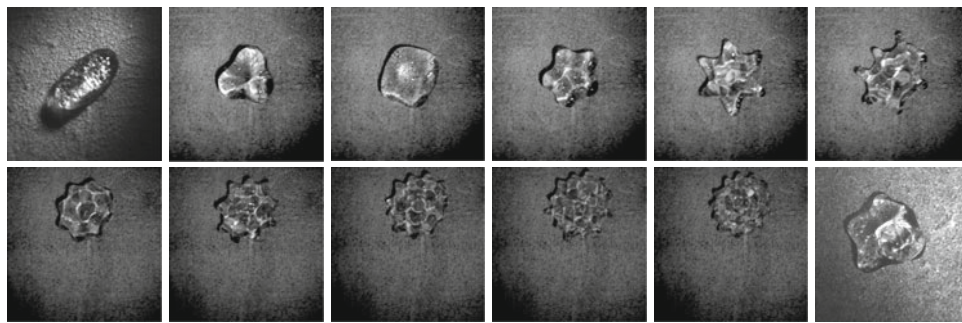


**Fig. 3.** Liquid drops ( $V = 500$  ml) adopting faceted shapes (stars) after being put on a shaken hydrophobic substrate. The snapshots show drops with 2 to 13 lobes, the number of lobes increasing with the prescribed frequency for the same drop volume. The last (bottom-right) shot shows a “chaotic” mode which results from the erratic combination of several modes.

These diagrams are reproduced in Figs. 4 and 5. The different colored symbols correspond to the threshold for the appearance of a star drop mode with  $n$  number of nodes in the azimuthal direction. At low acceleration, no instability appears whereas at high acceleration the drop can either take off the substrate (for smaller drops), either split into several smaller droplets (for larger drops). In between, stars such as those represented in Fig. 3 are observed.

The first striking impression is the complexity of the diagrams, especially for intermediate volumes ( $V = 200$  and  $500$  ml). This complex behavior is due to several factors: (1) The finite size of the drop leads to a constraint on the azimuthal wave-number, as the number of nodes has to be integer. The wave-number is not necessarily compatible with the frequency of excitation. (2) The drop can react preferentially to certain frequencies of excitations, due to the discrete values for the resonance peaks depending on the drop size. (3) The liquid viscosity is a damping factor, which is more and more prevalent as  $f$  is increased (see also [27]).

On the diagrams, the number of nodes inside the corresponding domains are written, and we also wrote the states denoted as “Chaos” where the coexistence between two or several modes leads to an undefined (or fluctuating) number of nodes (see Fig. 3, Bottom-Right shot). The general structure of the diagram is an ensemble of entangled and interconnected tongues of stability for various number of lobes  $n$ , which is reminiscent to what was obtained in the case of a droplet on a vibrating bath of the same liquid [22]. It is interesting to draw an analogy with the results for the (presumably) simpler system of a liquid layer exhibiting standing waves when shaken vertically: the so-called Faraday instability is also induced by parametric forcing. The linear stability theory of Faraday instability of a viscous fluid layer has been carried out by Kumar and Tuckerman [27], and a system of stability tongues in the space of wave-number and acceleration was predicted. In the case of a confined geometry, that is more similar to that of a drop, a system of sub-tongues is theoretically predicted and measured [28, 29], due to the constraint imposed by an integer number of waves at the surface. The superposition of the different stability tongues in our diagrams have similar features that require a more thorough investigation. We can extract several trends from the diagrams, which are summarized here:

- The threshold for the appearance of the first instability generally increases with the frequency, although not always in a monotonic way.
- The selected wave-number increases with the frequency. But there are generally several tongues of stability for the same number of nodes, which are disconnected.

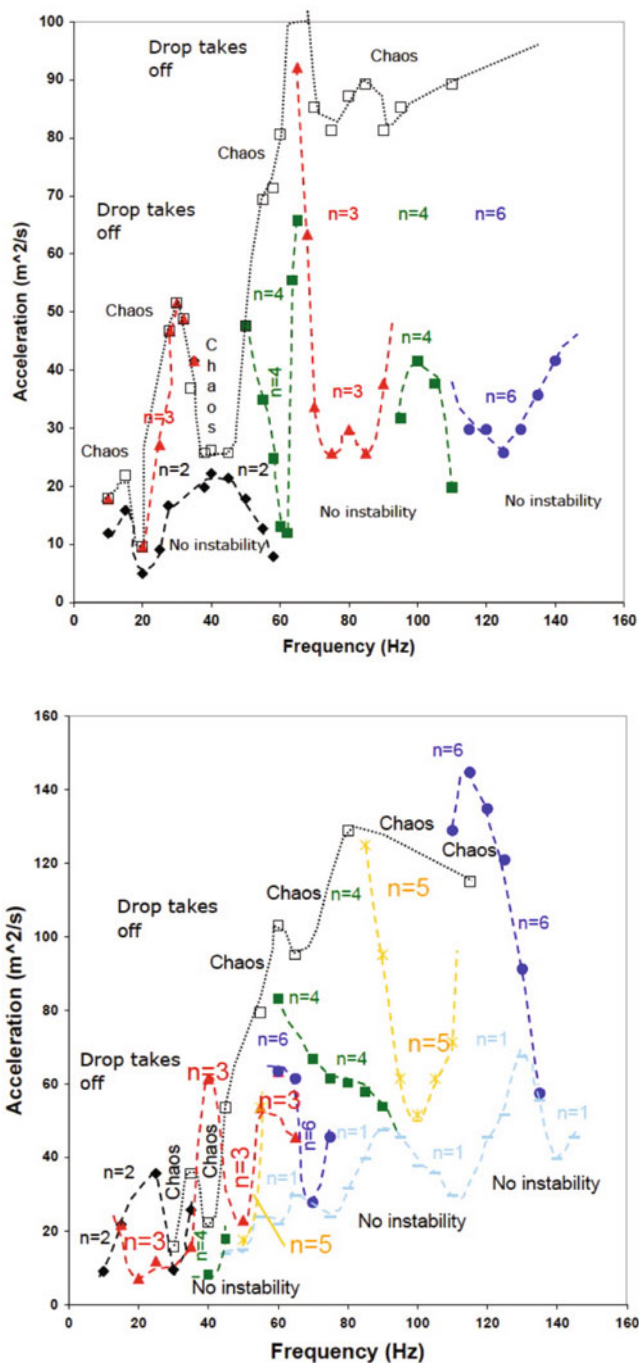


**Fig. 4.** The phase diagram in frequency and acceleration of a liquid puddle drop shaken on a non-wetting substrate *Left* -  $V = 100$  ml, *Right* -  $V = 200$  ml.

Between these tongues at constant  $n$ , other tongues corresponding to other values of  $n$  are selected.

- The chaotic regime generally appears for values of the acceleration higher than those required to observed regular stars at constant  $n$ . However, in some situations

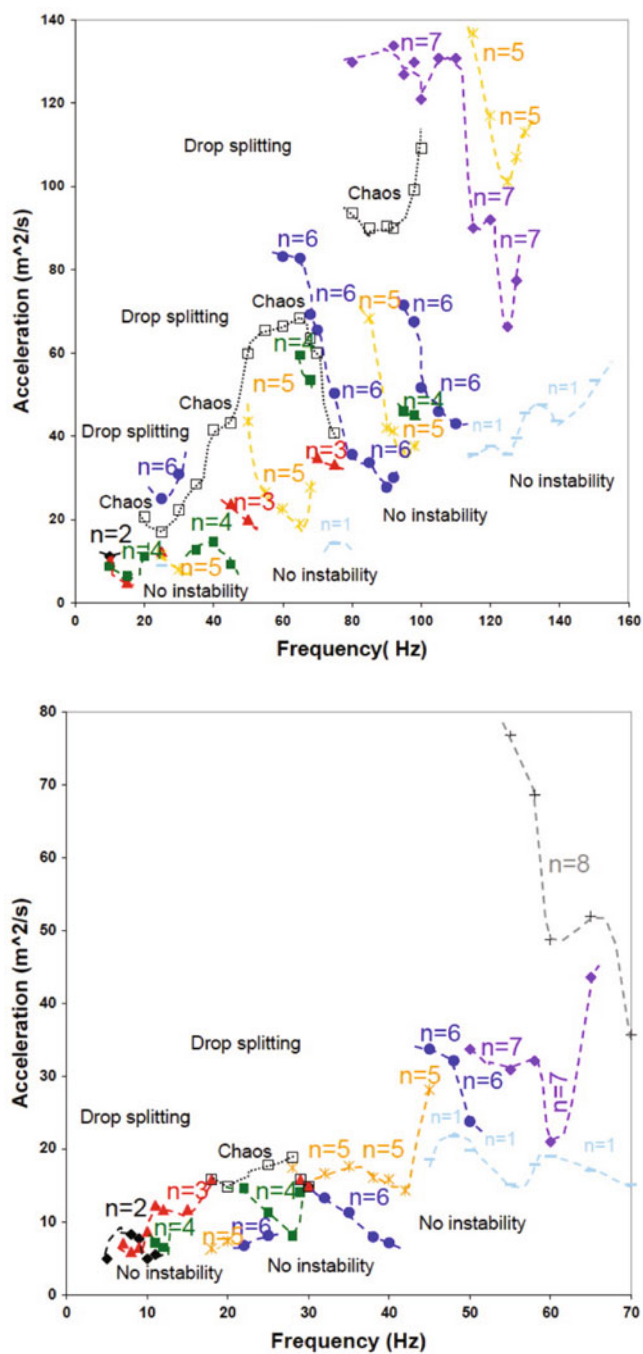


**Fig. 5.** The phase diagram in frequency and acceleration of a liquid puddle drop shaken on a non-wetting substrate. *Left* -  $V = 500$  ml, *Right* -  $V = 1000$  ml.

the chaos regime is between two tongues of stability and it is possible to re-observe a regular mode at higher accelerations: for instance for  $f_e$  around 40 Hz and  $n = 3$  at  $V = 200$  ml, or for  $f_e$  about 100 Hz and  $n = 7$  at  $V = 500$  ml.



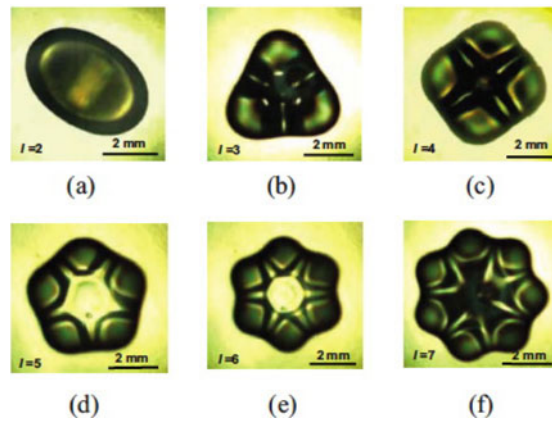


**Fig. 6.** Star drops generated in acoustic levitation, where the prescribed acoustic field is modulated in time at low frequency. Reprinted figure with permission from [30].

- The area of stability generally increases for larger  $n$ . For instance, the areas of stability of  $n = 2$  and  $n = 3$  are quite narrow, except for the smallest drop of  $V = 100$  ml.
- The mode  $n = 1$  does not correspond to a parametric forcing, but it can sometimes be observed between the “No instability” area and the tongues of stability of stars. Therefore, it is always stable at accelerations lower than those for  $n \geq 2$ .

### 2.3 Acoustic levitation

Recently, Chen, Xie and Wei [30] have set-up an experiment of acoustic levitation where a drop is put in an ultrasonic acoustic field (frequency  $f_0 = 20$  kHz). As the drop is trapped by acoustic radiation pressure, this acoustic force acting on the liquid/gas interface can counterbalance gravity and hence the drop can be kept in levitation. The drop is large compared to the capillary length  $l_c$ , so that it adopts the shape of a puddle, and not that of a sphere. This set-up can be particularly adapted to situations where contact between liquid and solid has to be avoided, for instance undercooled or reactive melts [30].

When the acoustic field is modulated in time, at a modulation frequency  $f_m$  much smaller than  $f_0$  – typically from 20 to 150 Hz, the authors observed star drops, with a number of lobes  $n$  between 2 and 7 depending on the modulation frequency, see Fig. 6. Therefore, a natural explanation of the phenomenon can be the following: the modulation of the acoustic power induces a modulation in the force that maintains the drop in levitation, and hence the drop’s vertical position fluctuates at the frequency  $f_m$ . This situation is very similar to that of a puddle on a vibrated substrate is set up. However, the acoustic levitation offers an even more symmetric situation: while a drop on a vibrated substrate is flattened at its lower base by the proximity of the substrate, a drop in acoustic levitation is up/down symmetric.

### 2.4 Metal drops in oscillating magnetic field

Fautrelle, Etay and Daugan [31] have observed very similar stars with a drop of quicksilver put in an magnetic field that is modulated at low frequency (about 1 to 10 Hz). These much smaller values for the frequency are explained by that the radius of the drop – denoted as “liquid pool” by the authors – is larger than that of other situations:  $R$  ranges between 1.5 and 2 cm. Furthermore, the ratio  $\frac{\gamma}{\rho}$  is much

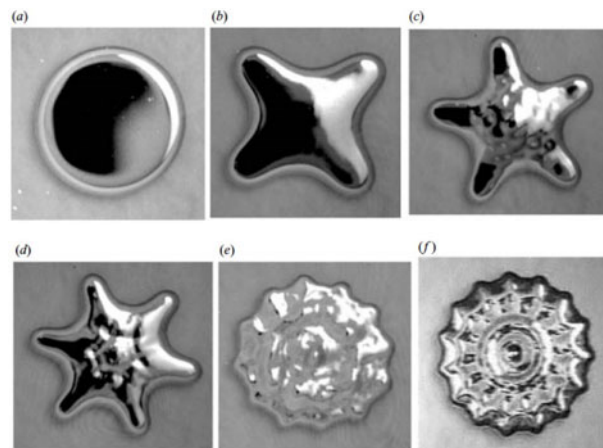


**Fig. 7.** Star drops of quicksilver generated in an oscillating magnetic field. Reprinted figure with permission from [31].

smaller here than for usual liquids due to the high density, which leads to even smaller eigen frequencies according to eq. (2). Figure 7 shows examples of such liquid metal stars. Similarly to the previous situations, the number of lobes  $n$  increases as one increases the frequency of the magnetic field modulation. The authors also mentioned the existence of the axisymmetric mode (snapshot (a) in Fig. 7), where  $n = 1$ , in a significant range of parameters. This mode is very similar to that observed for drops on a non-wetting vibrating substrate (sections 2.1 and 2.2), i.e. consisting of surface waves propagating inwards from the drop periphery.

It is also noticeable that unstructured patterns of waves were observed, with a host of various shapes for the drop. In these drops, some of which can resemble chaotic drops shown in Fig. 3, the number of lobes varies erratically over time and no well-defined wavelength can be observed. In their extreme shapes, these unstructured patterns can exhibit voids (absence of liquid) which position fluctuates in the middle of the drop, as well as ejections of small droplets.

## 2.5 Drops levitated by a pulsating air flow

Starting again from the issue of setting up containerless measurements on liquids, Papoular and Parayre [32] carried out experiments of oscillating drops on a porous substrate whereby an air stream flows. The air flow reaches the drop and acts as a bearing, hence insulating it from the substrate. The levitation is due to the lubrication flow in the air layer below the drop, which balances gravity. Therefore, this set-up allows to avoid contact between the liquid and the substrate, which ensures a very small friction. A piezoelectric exciter set below the cushion ensures the time-modulation of the air flow, hence leading to periodic excitation of the drop.

Figure 8 shows two examples of oscillating drops (side views) obtained with this set-up. The authors have focused their study on the determination of corrections to be brought to the Rayleigh-Lamb theory (eq. (2)), in the situations where the shape of the drop at rest is different from spherical. Therefore, the shape of their drops is elliptical, flattened by gravity at the lower base, but it is not a puddle. Consequently, the periodic excitation produces parametric instability, but the subsequent drop shapes are not star-like: the lobes and nodes develop along the up-down direction (see fig. 8).

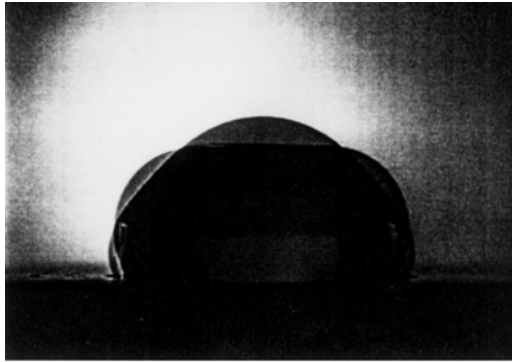


**Fig. 8.** Drop on a pulsating air flow, showing shape oscillations that remain axisymmetric. Reprinted figure with permission from [32].

### 3 Star drops levitated by a non-pulsed air cushion

So far, we presented formation of star or faceted drops that were subjected to a prescribed periodic forcing. But there are a few situations where star drops are observed *without periodic forcing*. Therefore, the vibrations come from an instability in the flow required to keep the drop in a non-wetting situation. Indeed, if one ensures the presence of an air cushion between the liquid and the substrate, a perfectly non-wetting situation is created. The contact angle is rigorously equal to  $180^\circ$  and the friction is almost zero. The levitation is ensured by a lubrication pressure due to the radial air flow, which balances gravity forces on the drop. This situation is observed at least within two sorts of experiments:

- A drop of liquid on a substrate which temperature is far beyond the liquid boiling temperature  $T_b$ , generating a situation of "boiling crisis" or Leidenfrost effect [34]. In this case, the vapor cushion comes from the evaporation of the liquid of the drop itself, that vaporizes fast enough to lift the drop up the surface and insulate it from the hot plate, making the drop evaporation much slower and less explosive than in boiling [37].
- A drop of liquid on a (porous) substrate through which an ascending air stream flows, generating a radial flow below the drop.

These two situations are depicted in Fig. 9. The average thickness of the air layer has been measured to be of the order of 100 microns or less [37].

#### 3.1 Leidenfrost star drops

The Leidenfrost effect is known since the 18<sup>th</sup> century, discovered by the german scientist who gave the name of the phenomenon [34]. However, the observation of vibrating Lendenfrost drops and the subsequent stars were first reported in the early fifties by Holter and Glasscock [15], with a tentative theoretical explanation by Gouin and Casal [35]. Many quantitative studies of the boiling crisis have focused on the determination of the Leidenfrost critical temperature, i.e. the temperature above which the lifetime of a drop dramatically increases, as boiling disappears (see [36] for a review). In many applications like quench-cooling, the boiling crisis has to be avoided as it strongly limits heat transfer between the solid to be cooled and the surrounding liquid. Recently, Biance et al. [37] investigated Leidenfrost drops in permanent regime, i.e. by feeding drop with water at the same rate as evaporation, and

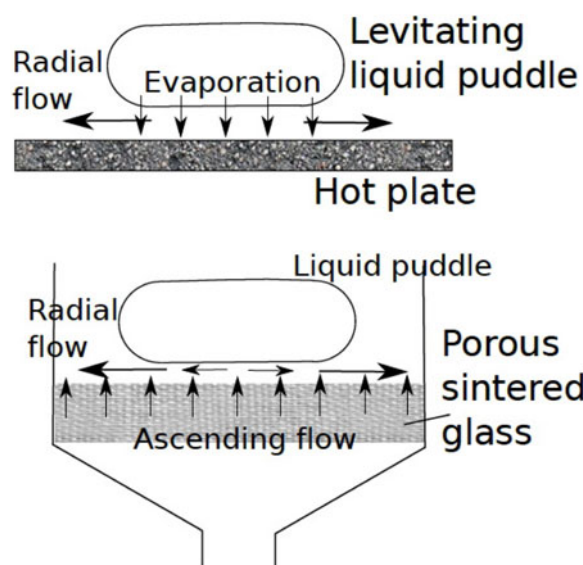


**Fig. 9.** Schemes of the two situations of levitating star drops on non-pulsed air cushions. *Top* - Leidenfrost drop on a hot plate. *Bottom* - Drop levitating by an ascending air stream.

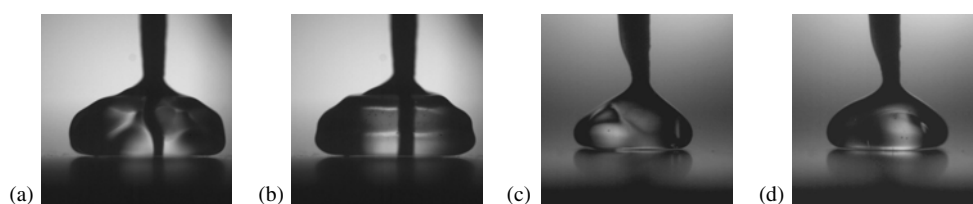


**Fig. 10.** Facetted drops of water sitting on a metallic hot plate, producing a vapor cushion (Leidenfrost effect). (a) Axisymmetric drop with propagating surface waves. (b) Facetted drop (four lobes) as the plate temperature is increased further. (c) and (d) A drop with 3 lobes spinning along the azimuthal direction. A needle is used to hold the drop in place.

focused on the vapor layer. They did observe drop vibrations leading to stars as well as a ‘chimney’ instability. The latter is manifestly different from the star instability, and occurs as the drop exceeds a certain size. The authors attributed these chimneys to the growth and rise of a vapor bubble at the centre of the drop, due to Rayleigh-Taylor instability [37].

Figure 10 shows a few examples of vibrating Leidenfrost drops of water and isopropanol on a hot plate (temperature  $T$  about  $220^\circ\text{C}$ ). There are a number of experimental challenges that make it difficult to obtain reproducible experimental data. The main issue is to carefully control the roughness of the substrate, which seems to have a large influence on the stability of the vapor layer [36]. Furthermore, in order to prevent the drop to slide off the plate, either the substrate has to be curved – which can bring an additional geometric parameter – either the drop has to be pinned by a thin needle on a flat plate (Fig. 10) the influence of which is quite unquantifiable. Finally, operating at constant local temperature for the plate is also an issue. Therefore, the alternative solution of operating in ambient conditions with liquid nitrogen has been adopted by many experimentalists.

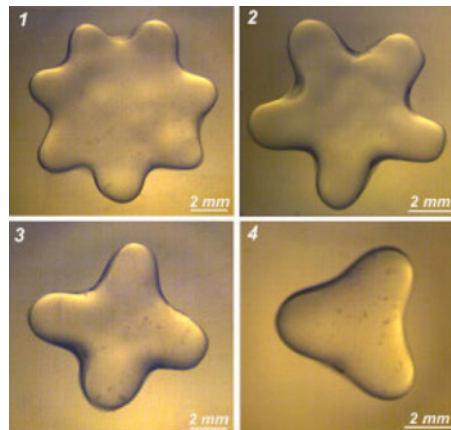


**Fig. 11.** Star drops of liquid nitrogen sitting on a layer of glycerol, hence developing a Leidenfrost state. Reprinted figure with permission from [18].

### 3.2 “Cold” Leidenfrost stars

Most of the quantitative experiments of vibrating Leidenfrost drops were conducted with liquid nitrogen on a substrate at ambient temperature. The main reason for this is that the substrate can be a liquid, which ensures more reproducible experiments: not only the liquid constitutes a perfectly smooth substrate at the molecular scale, but also its surface deforms under the weight of the levitating drop, ensuring that the drop stays trapped at a given location. In order to avoid flow inside the liquid substrate [18], the liquid has to be very viscous, yet thermally conductive enough. Figure 11 gives examples of such regular liquid nitrogen stars on glycerin pools.

The first quantitative studies were carried out by Adachi and Takaki [13, 14], which revealed a very rich dynamics including non-trivial transitions between the different spatial modes. They provided a tentative mechanism for the mode selection, that compared well with experiments. Later on, Strier et al. [16] reconsidered the results in terms of amplitude equations. Recently, Snezhko et al. carried out a new series of experiments and showed that the internal flows inside the liquid substrate could lead to different dynamical regimes. It was proposed that the vibrations could originate from thermal effects: these interpretations were supported by a linear stability analysis [17] and by direct visualization of thermal-convection like flow inside the drop [16]. This mechanism predicts a time-periodic variation of the radius of the drop, hence ensuring the conditions for parametric forcing (see Section 2.1).

An alternative explanation for the oscillations can invoke a purely hydrodynamic, non-thermal, mechanism. This scenario is supported by the observation of stars in athermal experiments, where a drop is simply put in levitation above an ascending air stream, which are reviewed and described thereafter.

### 3.3 Oscillating star drops on a constant ascending air stream

To our knowledge, the occurrence of oscillations of drops levitating on a constant ascending air stream has first been reported by Goldshtik, Khanin and Ligai [19], who drew an analogy between the air flow lubrication and the boiling crisis. Later on, Hervieu et al. [12] carried out a numerical study of the problem, which exhibited realistic shapes and oscillations of the center of mass<sup>1</sup>. They also checked

<sup>1</sup> As the numerical scheme was axisymmetric, it was unable to reproduce stars.

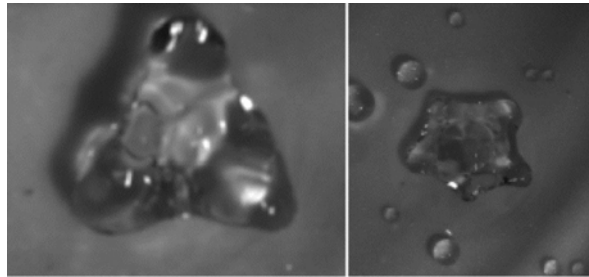


**Fig. 12.** Star drops obtained on an air cushion formed above a porous mould, here with 3 or 5 lobes.

experimentally the existence of such oscillations, with a few results comparing well with numerics.

### 3.3.1 General features

To levitate a drop on a porous mould intervenes in several practical situations like the manufacture of lenses, for which it is crucial to avoid shape instability in the drop of liquid glass. As summarized in Duchemin, Lister and Lange’s paper [10], instabilities can occur due in the coupled system of air flow and drop, leading to the oscillations of the drop shape. Several kinds of instabilities have been reported:

- the growth and rise of a bubble below the drop, which ends up piercing on top of the drop. This is reminiscent to the “chimneys” observed by Biance et al. [37] in Leidenfrost drops.
- the appearance of static “brim waves” [10], i.e. small deformations at the edge of the drop.

None of these two instabilities have been proposed to possibly lead to star drops. We know that liquid stars should appear as soon as the drop’s center of mass oscillates vertically with a high enough amplitude, and it is not possible to conclude whether one of mechanism described in [10] can generate the required oscillations. However, according to the conclusions of Goldshtik et al., star drops should in principle be possible to observe on an air cushion as the flow produces the required vertical oscillations for the drop. This is what we checked experimentally, and it turned out that indeed a drop of liquid levitating on top of a air cushion did show star shapes (see Fig. 12).

We recently conducted a theoretical study to predict the maximal size of a drop on an air cushion [20]. This study was based on solving the shape of the drop/air interface using lubrication approximation, i.e. neglecting the inertia in the air flow. This was justified by the very realistic shapes obtained, as well as by the simplifications in the theoretical and analytical treatment. Analytical predictions for the shape based on asymptotic matching could be obtained, and numerical computations were additionally run to capture the transient dynamics of unstable drops. The main conclusions of the study in relation to the oscillating drops, are summarized here:

- A solution exists for drops up to a certain external radius which is in very good agreement with experiments by Biance et al. [37]. Indeed they observed the appearance of chimneys above a drop radius equal to about 4 times the capillary length.

- The model predicts that a bubble grows and rise at the center of the drop, forming a chimney, if the radius is larger than the threshold radius. This threshold is dependent on air flow-rate: a larger flow-rate lowers the maximal radius that a stable drop can adopt.
- The presence of a curved substrate enhances stability of large drops.
- The lubrication flow alone is unable to reproduce drop oscillations.

Therefore, if one wishes to explain the occurrence of periodic vertical vibrations of the drop leading to star shapes, one cannot account on a simple balance between the lubrication pressure driven by the radial air flow and the Laplace pressure induced by the drop deformation at its lower base. Before conjecturing some possible mechanisms, we present new experimental results of drops levitated by an air cushion which show oscillations and star shapes.

### 3.3.2 First experiments

A schematic view of the experimental set-up is described in Fig. 9. An air stream flows through a porous substrate made of sintered glass, and keeps in levitation a drop of water placed above. Due to the very low friction, it is necessary to keep the drop pinned by a thin needle (0.35 mm thin). This needle is connected to a syringe which is used to control the drop volume. The air flow is produced by a pressurized air supply, which can maintain pressures up to 4 bars. The flow-rate  $Q$  is measured by a float flow-meter. The drop is observed from above by a high-speed camera (Photron SA3).

The main difficulty of the experiment is to have a robust hydrophobic chemical treatment of the porous medium. Indeed to set up drop levitation experiments is tricky because any contact between the liquid drop and the porous substrate has to be avoided. On that purpose, we chose perfluorodecyltrichlorosilane, which is a low surface-energy molecule, as a chemical coating that ensures a molecular monolayer on the activated glass porous layer. In the case of liquid contact and intrusion into the porous substrate, the quality of the water-repellent character is dramatically reduced, even after extensive drying, making the experiments even more difficult. Practically, with the best care devoted to protect the coating, we could carry out experiments during two days without observing irreversible damage of the porous material.

It was possible to obtain some results demonstrating the appearance of liquid stars, very similar to those observed in the Leidenfrost configuration. Examples of such stars are illustrated in Fig. 13, where modes  $n = 3$  and  $n = 4$  are presented.

By taking water drops of different volume  $V$  and radius  $R$ , we measured the conditions for a drop to be stable. It turns out that below a threshold in air flow-rate  $Q_c$ , a drop of given radius does not show oscillations and adopts a smooth spherical or puddle shape. We measured the threshold  $Q_c$  which is larger for smaller drops. In other terms, larger drops are more susceptible to get destabilized. This is consistent with the results of the study in [20]. The destabilization always starts with fast capillary waves (of frequency about a few hundred Hertz) at the surface of the drop. Then, the drop undergoes more dramatic changes and turns to faceted and stars shapes like those shown in Figs. 12 and 13. Figure 14 summarizes the various observed drop shapes: while small drops gets unstable by taking the shape of stars ( $n = 3$  for the smallest diameters,  $n = 4$  or 5 for slightly larger drops), the largest drops get destabilized by the occurrence of chimneys, which do not turn the drop's shape into a star but simply break the upper interface. The theoretical limit of stability for drops at low flow-rate should be equal to about 4 times the capillary length [20]. This limit is traced in red dotted line in Fig. 14, which is in good agreement with the extrapolation of the experimental measurements to  $Q = 0$ .

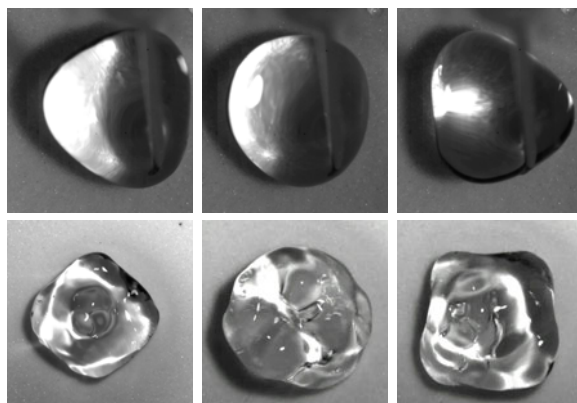


**Fig. 13.** Vibrations and subsequent faceted shapes on water drops sitting on an air cushion. *Top* - A mode  $n = 3$ . *Bottom* - A mode  $n = 4$ .

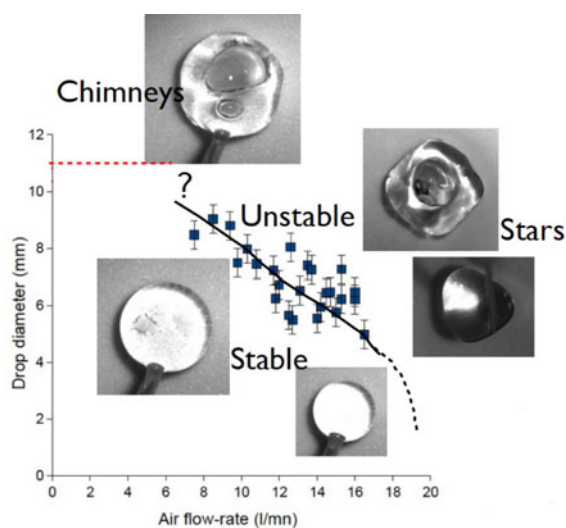


**Fig. 14.** The limit of air flow-rate and drop diameter that separates stable and unstable drops, showing that smaller drops turn unstable at smaller air flow-rate.

We checked experimentally that the measured frequencies of the stars correspond to those predicted by the eq. (4):

- for the  $n = 3$  stars (Fig. 13-Top), the measured frequency is 58.5 Hz, whereas the frequency predicted from eq. (4) is  $f_{th} = 52.9$  Hz (the drop radius is measured equal to 2.52 mm). It is to be noticed that the eq. (2) for spherical drops give a better prediction with  $f_{th} = 56$  Hz, presumably because this small drop is closer to a sphere than to a puddle (see Fig. 13-Top).
- for the  $n = 4$  stars (Fig. 13-Bottom), the measured frequency is 31 Hz, which is in good agreement with the frequency predicted from eq. (4) is  $f_{th} = 30.3$  Hz (the drop radius is measured equal to 4.95 mm).

This quite satisfactory agreements are encouraging for more systematic measurements of the selected frequency for different flow-rate  $Q$ , which should give the relationship between  $Q$  and the frequency of the vertical oscillation of the drop, equal to twice the



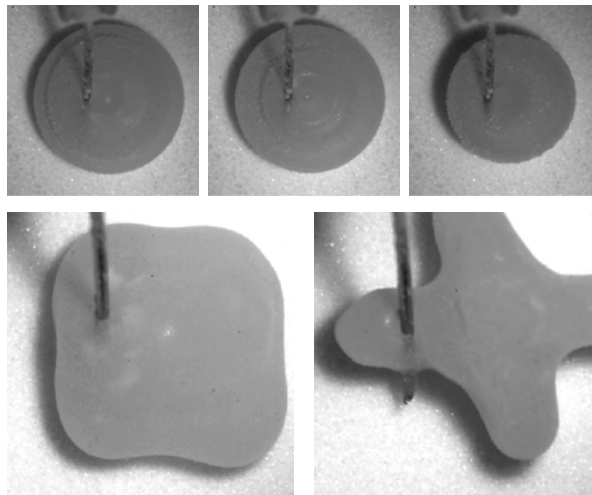


**Fig. 15.** Vibrations of a liquid marble, a drop coated by hydrophobic powder, sitting on an air cushion. *Top* - Axisymmetric waves propagating inwards ( $n = 1$ ). *Bottom* - Examples of a faceted liquid marble ( $n = 4$ ).

measured frequency of the stars according to the mechanism of parametric instability presented in Section 2.1.

### 3.3.3 Levitation and faceting of liquid marbles

Due to the short lifetime of the current available hydrophobic coating, we carried out experiments by coating the drop itself with hydrophobic particles. Using such coated drops efficiently prevents any liquid/substrate contact, as the particles self-assemble at the liquid surface and constitute a robust “skin”. These drops have been denoted as “liquid marbles” in the literature and have first been studied by Aussillous and Quéré [38]. Later on, several authors have attempted to measure their effective surface tension through their dynamical properties [39,40].

Figure 15 shows two examples of dynamical modes generated by vertical oscillations. The mode  $n = 1$  (on top of the figure) seems to be much more stable than for usual levitating liquid drops, and could be observed during several seconds. This mode consists of surface waves propagating inwards, without azimuthal corrugation. Despite the vertical oscillations and the time-periodic fluctuations of the radius, the drop stays symmetrical as the amplitude of the vertical vibrations are too weak to induce parametric forcing. The unusual stability of the mode  $n = 1$  could be explained by the additional dissipation due to the presence of particles on the drop interface. It is important to note that the eigen frequency of this mode  $n = 1$  cannot be predicted by eqs. (2) and (4).

Besides, we observed more usual modes with  $n = 3, 4$  or  $5$  (bottom of Fig. 15). From our experimental observations, it turns out that the mode selection is not very regular: the number of lobes fluctuates over time, as the occurrence of a selected mode generally lasts no longer than a few periods. This chaotic behavior could not be tamed, and it is presumably due to the uneven shape of the interface of the coated drop. Nevertheless, this is encouraging for future experiments because it was possible to obtain star drops with much larger puddles than for simple water drops, and also to evidence that the transition from a mode  $n = 1$  to modes with several lobes occurs above a certain threshold in air flow-rate.

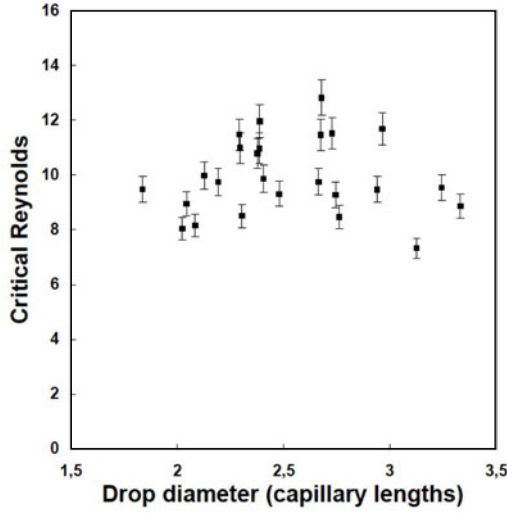


**Fig. 16.** Critical Reynolds number vs. diameter for the destabilization of the drop.

### 3.4 The underlying mechanism of oscillations?

The fact that stars drops also appear when levitated by an air cushion suggests that the thermal effects present for Leidenfrost drops are not crucial for the star formation. We therefore look for a hydrodynamic mechanism that generates the oscillations. In principle, one would need to solve the stability of the air flow below the drop, coupled to the flow inside the drop. It is not possible to conjecture *a priori* whether or not the inner flow of the drop is involved in the instability process. The theoretical study conducted in [20] showed that no oscillations can appear from a purely visco-capillary treatment of the air flow below the drop. Hence, one may expect inertia to be important. Let us therefore consider the Reynolds number in the air layer, which quantifies the relative importance of inertial and viscous forces:

$$Re = \frac{U \times h}{\nu} \quad (6)$$

where  $\nu$  is the kinematic viscosity of air,  $U$  is the mean radial velocity and  $h$  is the average thickness. The radial flow is a direct consequence of the ascending air stream below the drop. Therefore, the product  $U \times h$  can be evaluated by mass conservation, considering that all the ascending air flowing through the porous surface in the area below the drop is conserved in the flow leaving radially the drop.

$$Q \frac{d_D^2}{d_P^2} = \pi d_D U(R) h(R) \quad (7)$$

where  $d_P$  and  $d_D$  are the diameters of the porous substrate and of the drop, and  $R = \frac{1}{2}d_D$ . Knowing the global flow-rate  $Q$ , it is easy to calculate the Reynolds number by taking  $U \times h$  at the periphery of the drop ( $r = R$ ). From the critical flow-rate measurements of Fig. 14, we can plot the critical Reynolds number for the appearance of unstable drops. Figure 16 show the results versus the dimensionless drop diameter  $\frac{d_D}{l_c}$ : the critical Reynolds number is not far from being constant at the transition, with values ranging from 8 to 12.

These results suggest that the instability appears when inertia in the air flow is significant enough. Other dimensionless numbers like the Reynolds number in the

liquid drop, or the Weber number (ratio between inertia and capillarity) do not show such trend at the transition.

## 4 Conclusions – Open points and perspectives

In this short review, we presented various situations where large drops can develop time-periodic standing waves in their azimuthal direction, giving them the shape of a star. This instability occurs subsequently to a parametric forcing that originates from the time-periodic fluctuations of the drop radius, generally induced by an oscillating acceleration field. We have shown that this situation could be obtained in many experimental set-ups, some of which have been imagined for practical purposes like the handling of corrosive or supercooled fluids. The creation of such stars induces inner flow which is suitable for mixing.

We also presented preliminary experiments that showed for the first time that star drops can be generated above non-pulsed air cushions. In this latter case, an instability in the air layer occurs above a threshold in Reynolds number of about 10, suggesting that an inertial mechanism takes place in the instability process. The vibration frequency is once more compatible with Rayleigh-Lamb modes, so it will be crucial to determine the vertical frequency of oscillations to propose a detailed mechanism. Note that these experiments show that thermal effects (as present in the Leidenfrost drops) are not necessary to generate the instability towards star drops.

A possible way to answer the remaining unsolved questions about the instability process, would be to carry out levitation experiments with highly viscous liquids. Duchemin et al. [10] mention that chimneys or brim waves are observed in a drop of viscous molten glass, but there was no mention of stars. Experiments of levitation were carried out with a solid plastic disk of about the same size of drops and density comparable to water, and no vertical oscillations could be observed (see also [41]). One of the remaining question is then: are oscillations and subsequent stars only due to the deformable character of the liquid drop<sup>2</sup>, or does the mechanism also involve the inner flow of the drop, where the liquid is sheared by the air stream? This last question points out that it could be possible to observe vertical oscillations due to the air flow instability, without necessarily inducing stars or faceted shapes (which generation is hindered by a large viscosity). Indeed, a significant inner flow is required to generate stars and the liquid viscosity could well damp the parametric forcing. The large range of stability of the axisymmetric  $n = 1$  mode (i.e. vertical oscillations without stars) noticed for the levitated liquid marbles, is a clue that goes in this sense.

It is a pleasure to thank Basile Pottier for his significant contribution to the experiments of levitating drops. Nhung T.P. Nguyen is kindly acknowledged for her support and help in the surface treatment of the porous substrate.

## References

1. H. Lamb, *Hydrodynamics* (Cambridge University Press, Cambridge, UK, 1932)
2. A.J. James, B. Vukasinovic, M.K. Smith, A. Glezer, *J. Fluid Mech.* **476**, 1 (2003)
3. X. Noblin, A. Buguin, F. Brochard-Wyart, *Eur. Phys. J. E* **14**, 395 (2004)
4. X. Noblin, A. Buguin, F. Brochard-Wyart, *Phys. Rev. Lett.* **94**, 166102 (2005)

<sup>2</sup> In this case, the vertical oscillations would appear in a mechanism analogous to that of some wind musical instruments, like the clarinet, where constant air flow through a narrow space induces vibrations of the flexible reed and produces the sound.

5. N. Yoshiyasu, K. Matsuda, R. Takaki, J. Phys. Soc. Jpn. **65**, 2068 (1996)
6. P.G. de Gennes, Rev. Mod. Phys. **57**, 827 (1985)
7. S. Courty, G. Lagubeau, T. Tixier, Phys. Rev. E **73**, 045301(R) (2006)
8. F. Celestini, R. Kofman, Phys. Rev. E **73**, 041602 (2006)
9. V. Palero, J. Lobera, P. Brunet, M. Pilar Aroyo (in preparation)
10. L. Duchemin, J.R. Lister, U. Lange, J. Fluid Mech. **533**, 161 (2005)
11. P.H. Hausmesser et al., Rev. Sci. Instr. **73**, 3275 (2002)
12. E. Hervieu, N. Coutris, C. Boichon, Nucl. Eng. Design **204**, 167 (2001)
13. K. Adachi, R. Takaki, J. Phys. Soc. Jpn. **53**, 4184 (1984)
14. R. Takaki, K. Adachi, J. Phys. Soc. Jpn. **54**, 2462 (1985)
15. N.J. Holter, W.R. Glasscock, J. Acous. Soc. Am. **24**, 682 (1952)
16. D.E. Strier, A.A. Duarte, H. Ferrari, G.B. Mindlin, Physica A **283**, 261 (2000)
17. N. Tokugawa, R. Takaki, J. Phys. Soc. Jpn. **63**, 1758 (1994)
18. A. Snezhko, E. Ben Jacob, I.S. Aranson, New J. Phys. **10**, 043034 (2008)
19. M.A. Goldshtick, V.M. Khanin, V.G. Ligai, J. Fluid Mech. **166**, 1 (1986)
20. J.H. Snoeijer, P. Brunet, J. Eggers, Phys. Rev. E **79**, 036307 (2009)
21. Y. Couder, E. Fort, C.H. Gautier, A. Boudaoud, Phys. Rev. Lett. **94**, 177801 (2005)
22. S. Dorbolo, D. Terwagne, N. Wandewalle, T. Gilet, New J. Phys. **10**, 113021 (2008)
23. L. Rayleigh, *The Theory of Sound*, Vol. 1, 2nd edn. (New York, Dover, 1945), p. 81
24. M. Versluis, D.E. Goertz, P. Palanchon, I.L. Heitman, S.M. van der Meer, B. Dollet, N. de Jong, D. Lohse, Phys. Rev. E **82**, 026321 (2010)
25. M. Okada, M. Okada, Exp. Fluids **41**, 789 (2006)
26. X.-M. Li, D. Reinholdt, M. Crego-Calama, Chem. Soc. Rev. **36**, 1350 (2007)
27. K. Kumar, L.S. Tuckerman, J. Fluid Mech. **279**, 49 (1994)
28. S. Douady, J. Fluid Mech. **221**, 383 (1990)
29. M. Perlin, W.W. Schultz, Ann. Rev. Fluid Mech. **32**, 241 (2000)
30. C.L. Shen, W.J. Xie, B. Wei, Phys. Rev. E **81**, 046305 (2010)
31. Y. Fautrelle, J. Etay, S. Daugan, J. Fluid Mech. **527**, 285 (2005)
32. M. Papoular, C. Parayre, Phys. Rev. Lett. **78**, 2120 (1997)
33. M. Perez, Y. Brechet, L. Salvo, M. Papoular, M. Suery, Europhys. Lett. **47**, 189 (1999)
34. J.G. Leidenfrost, *De Aquae Communis Nonnullis Qualitatibus Tractatus* (Duisburg on Rhine, 1756)
35. P. Casal, H. Gouin, Int. J. Engng Sci. **32**, 1553 (1994)
36. J.D. Bernardin, I. Mudawar, Trans. ASME - J. Heat Transf. **121**, 894 (1998)
37. A.-L. Biance, C. Clanet, D. Quéré, Phys. Fluids **15**, 1632 (2003)
38. P. Aussillous, D. Quéré, Nature **411**, 924 (2001)
39. G. McHale, S.J. Elliott, M.I. Newton, D.L. Herbertson, K. Esmer, Langmuir **25**, 529 (2009)
40. E. Bormashenko, R. Pogreb, G. Whyman, A. Musin, Y. Bormashenko, Z. Barkay, Langmuir **25**, 1893 (2009)
41. E.J. Hinch, A. Lemaitre, J. Fluid Mech. **273**, 315 (1994)